

# Helical magnetorotational instability of Taylor-Couette flows in the Rayleigh limit and for quasi-Kepler rotation

G. Rüdiger<sup>?</sup> and M. Schultz

Astrophysikalisches Institut Potsdam, An der Sternwarte 16, D-14482 Potsdam, Germany

Received 2008 May 14, accepted 2008 Jul 2

Published online 2008

**Key words** turbulence – magnetohydrodynamics – magnetorotational instability

The magnetorotational instability (MRI) of differential rotation under the simultaneous presence of axial and azimuthal components of the (current-free) magnetic field is considered. For rotation with uniform specific angular momentum the MHD equations for axisymmetric perturbations are solved in a local short-wave approximation. All the solutions are overstable for  $B_z \neq 0$  with eigenfrequencies approaching the viscous frequency. For more flat rotation laws the results of the local approximation do not comply with the results of a global calculation of the MHD instability of Taylor-Couette flows between rotating cylinders. – With  $B_r$  and  $B_z$  of the same order the traveling-mode solutions are also preferred for flat rotation laws such as the quasi-Kepler rotation. For magnetic Prandtl number  $P_m \gg 0$  they scale with the Reynolds number of rotation rather than with the magnetic Reynolds number (as for standard MRI) so that they can easily be realized in MHD laboratory experiments. – Regarding the nonaxisymmetric modes one finds a remarkable influence of the ratio  $B_r/B_z$  only for the extrema. For  $B_r \ll B_z$  and for not too small  $P_m$  the nonaxisymmetric modes dominate the traveling axisymmetric modes. For standard MRI with  $B_z \neq 0$ , however, the critical Reynolds numbers of the nonaxisymmetric modes exceed the values for the axisymmetric modes by many orders so that they are never preferred.

© 2008 WILEY-VCH Verlag GmbH & Co. KGaA, Weinheim

## 1 Introduction

It has been shown in previous publications starting with Hollerbach & Rüdiger (2005) that the magnetorotational instability (MRI) under the presence of both current-free axial and azimuthal components of the magnetic field ('Helical' fields, hence HMRI) is always characterized by an eigenoscillation frequency. In combination with the vertical wavenumber the resulting instability pattern is thus an axisymmetric wave traveling along the rotation axis. In all our considerations the magnetic Prandtl number  $P_m$  plays the basic role. For  $P_m \gg 0$  the HMRI scales with the Reynolds number  $Re$  rather than with the magnetic Reynolds number  $R_m$  as it does for the standard magnetorotational instability for an axial magnetic field. The questions arise whether this frequency reflects the geometry of the magnetic field and whether it is observable with real astrophysical objects such as protoneutron stars and/or accretion disks. Also the relation to the Azimuthal MagnetoRotational Instability (AMRI, see Rüdiger et al. 2007b) for (current-free) toroidal fields which is nonaxisymmetric and which scales with the magnetic Reynolds number for  $P_m \gg 0$  must be considered. We find the AMRI only weakly (if ever) influenced by the addition of an axial field which is not much stronger than the toroidal field. For  $P_m \ll 1$  the difference between  $Re$  and  $R_m$  disappears so that the main differences of the instabilities also disappear.

In the present paper we start with a local approximation using analytical methods for the most simple rotation law for constant specific angular momentum, i.e. the Rayleigh limit. Global calculations of the stability of the same rotation law between two rotating perfect-conducting cylinders and threaded by a helical current-free magnetic field lead to an almost perfect coincidence of the results of both methods. This is no longer true, however, for more flat rotation laws such as quasikeplerian rotation in a finite gap where the differences of the short-wave approximation (which only holds for infinitely thin gaps) and global models are so strong that the results completely differ (Rüdiger & Hollerbach 2007).

## 2 Dispersion relation for very small gaps

The dynamics of conducting fluids is described by the MHD equations

$$\frac{\partial \mathbf{u}}{\partial t} + (\mathbf{u} \cdot \nabla) \mathbf{u} = \frac{1}{r} \nabla_{\perp}^2 \mathbf{u} + \frac{B_r^2}{2B_z} \nabla_{\perp}^2 \mathbf{u} + \frac{1}{B_z} (\mathbf{B} \cdot \nabla) \mathbf{B} + \nabla_{\perp}^2 \mathbf{u}; \quad (1)$$

$$\frac{\partial \mathbf{B}}{\partial t} = \text{rot}(\mathbf{u} \times \mathbf{B}) + \nabla_{\perp}^2 \mathbf{B}; \quad (2)$$

and  $\text{div} \mathbf{u} = \text{div} \mathbf{B} = 0$ : Here  $\mathbf{u}$  is the fluid velocity,  $p$  the pressure,  $\rho = \text{const}$  the density and  $\mathbf{B}$  is the magnetic field. In cylindrical symmetry this set of equations has the stationary solution  $\mathbf{B}_0 = B_r(R) \mathbf{e}_r + B_z \mathbf{e}_z$  where  $B_z$  is a constant and  $B_r = I/R$  is current-free except on the rotation axis.

<sup>?</sup> Corresponding author: ruediger@aip.de

Following Lakhin & Velikhov (2007) we start with a local analysis. The perturbations are assumed to be axisymmetric and proportional to  $\exp(\tau + ik_R R + ik_z z)$ , where  $\tau = i\omega$  with (the real part of)  $\omega$  as the eigenoscillation frequency and  $k = (k_R; 0; k_z)$  the wave number vector. The local short-wave analysis is justified when  $k_R \gg 1/R$ . Then the equations of small-amplitude perturbations of the steady-state flow  $u_0 = (v_R) e^{i\omega t}$  are

$$(i\omega + \nu k^2) u_R^0 - 2 \nu u^0 = ik_R \frac{P^0}{R} + \frac{i(k_B v_0)}{R} B_R^0 - \frac{B_0}{2R} B^0; \quad (3)$$

$$(i\omega + \nu k^2) u^0 + \frac{2}{R} u_R^0 = \frac{i(k_B v_0)}{R} B^0; \quad (4)$$

$$(i\omega + \nu k^2) u_z^0 = ik_z \frac{P^0}{R} + \frac{i(k_B v_0)}{R} B_z^0; \quad (5)$$

$$(i\omega + \nu k^2) B_R^0 = i(k_B v_0) u_R^0; \quad (6)$$

$$(i\omega + \nu k^2) B^0 = i(k_B v_0) u^0 + R \frac{d}{dR} B_R^0 + \frac{2B_0}{R} u_R^0; \quad (7)$$

$$k_R u_R^0 + k_z u_z^0 = 0; \quad k_R B_R^0 + k_z B_z^0 = 0; \quad (8)$$

Here  $\nu = \nu k^2$  is the viscous frequency,  $\nu = \nu k^2$  is the resistive frequency and the epicyclic frequency is

$$\nu = \frac{1}{R^3} \frac{d}{dR} \nu R^4; \quad (9)$$

$P^0$  is the total pressure perturbation. Then the dispersion relation

$$\begin{aligned} & [(i\omega + \nu k^2)(i\omega + \nu k^2) + \nu k_z^2] \nu k^2 - \nu k^2 \\ & \quad \times \left[ (i\omega + \nu k^2)^2 + \nu k_A^2 + \frac{\nu k_A^2}{i} (i\omega + \nu k^2) \right] \\ & \quad - \frac{\nu k_z^2}{k^2} [ \nu k_A^2 + i(i\omega + \nu k^2) \nu k_A ] [ \nu k_A^2 + i(i\omega + \nu k^2) \nu k_A ] \\ & \quad = 0 \quad (10) \end{aligned}$$

results with

$$\nu k_A^2 = \frac{(k_B v_0)^2}{R}; \quad \nu k_A^2 = \frac{B^2}{R^2}; \quad (11)$$

The local dispersion relation is an equation of fourth order for the frequency. In the two limiting cases when either  $\nu k_A^2 = 0$  or  $\nu k_A^2 = 0$  the coefficients in Eq. (10) are real. In general, however, the coefficients of the dispersion relation (10) are complex. To find the stability criterion the method by Elstner, Rüdiger & Tschäpe (1989) is applied. For ideal fluids Blokland et al. (2005) used a very similar approach.

### 3 Rotation with constant specific angular momentum (the Rayleigh limit)

For rotation with constant specific angular momentum we have  $\nu = 0$  which is called the Rayleigh limit in the Taylor-Couette community (see the MRI papers by Willis

& Barenghi 2002; Rüdiger, Schultz & Shalybkov 2003; Velikhov et al. 2006). One obtains from Eq. (10) the critical angular velocity

$$\omega_c = \frac{k^2 \nu}{2k_z^2 \nu k_A^2} \frac{F}{\nu k_A^2} \frac{\nu k_A^2}{(\nu k_A^2 + \nu k^2)^2 + 4(\nu k_z^2 = k^2) \nu k_A^2} \nu k_A^2; \quad (12)$$

with  $F = \nu k_A^2 + \nu k^2 + 2(\nu k_z^2 = k^2) \nu k_A^2$ : The frequency of marginally stable modes is

$$\omega = \nu k_A^2 \frac{(\nu k_A^2 + \nu k^2)^2 + 4(\nu k_z^2 = k^2) \nu k_A^2}{(\nu k_A^2 + \nu k^2)^2 + (\nu k_z^2 = k^2) \nu k_A^2} \nu k_A^2; \quad (13)$$

(Lakhin 2007, private communication). For a very weak azimuthal magnetic field the instability limit is then defined by

$$\omega_c = \frac{k^2 \nu}{4k_z^2 \nu k_A^2} \frac{1}{(\nu k_A^2 + \nu k^2)^2 + \frac{k_z^2}{k^2} \nu k_A^2} \nu k_A^2 \nu k_A^2; \quad (14)$$

Obviously, when the condition

$$2(\nu k_A^2 + \nu k^2) < (\nu k_A^2)^2 \quad (15)$$

is fulfilled the azimuthal magnetic field supports the instability. Hence, the destabilizing effect of  $B_z$  disappears for  $Pm = 1$  but it also exists for  $Pm > 1$ .

With the free parameter  $\nu k_z^2 = k^2$  and with

$$\frac{\nu k_A^2}{\nu k_A^2} = Ha = Ha; \quad (16)$$

one finds from (12) and (13)

$$\frac{\omega}{\nu k_A^2} = 2 \frac{\nu k_A^2 \nu k_A^2}{F} \quad (17)$$

and  $F = \nu k_A^2 + \nu k^2$  for weak magnetic fields. Then

$$\frac{\omega}{\nu k_A^2} = 2 \frac{\nu k_A^2 \nu k_A^2}{\nu k_A^2 + \nu k^2} \nu k_A^2; \quad (18)$$

Hence, the oscillation frequency results from the simultaneous existence of  $\nu k_z^2$ ;  $B_z$  and  $B$  (Knobloch 1996). It exists despite of  $\nu = 0$ . The magnetorotational instability with helical but current-free magnetic fields is characterized by the existence of a frequency which only for the special case  $B = 0$  vanishes (see also Blokland et al. 2005). As the simultaneous existence of poloidal and toroidal components of the magnetic field is quite characteristic for cosmic objects one could expect that the observation of the eigenfrequency may serve as the proof of the existence of the MRI ('magnetoseismology', see Blokland et al.).

In the following the pitch angle

$$= \frac{B}{B_z} \quad (19)$$

is used, and we write  $\omega = k_z R$  and

$$Re = Re = \frac{c}{!} ; \tag{20}$$

Equations (12) and (13) then lead to

$$\frac{!}{c} Re ' ; \tag{21}$$

meaning that

$$! ' ! \tag{22}$$

for the marginal stable mode (Lakhin & Velikhov 2007). Obviously, even a small viscosity proves to be important for the system. Computations on the basis of the dispersion relation (25) under neglect of the viscosity (Liu et al. 2006) cannot lead to the same conclusion. With the renormalization

$$! = \frac{!}{P \frac{!}{!}} ; \tag{23}$$

one finds

$$! ' \frac{P}{Pm} ; \tag{24}$$

independent of  $\beta$ . At the Rayleigh limit it is thus the viscosity frequency which is emanated by the MHD system.

We shall show that this relation indeed is valid for the rotation law fulfilling the Rayleigh condition, i.e.  $\omega / R^2$ . It remains true for both local and global calculations. Though, for more flat rotation profiles (such as the Kepler law  $\omega / R^3=2$ ) the situation becomes more and more complicate, and the oscillation frequency starts to run with the Alfvén frequency  $\omega_A$  of the axial magnetic field (but not with the pitch angle  $\beta$ ). Differences between the local and the global results become more and more large, only the Pm-dependence of the characteristic frequency remains weak.

### 4 The numerical method

A numerical method to solve the dispersion relation has been developed. The dispersion relation reads

$$\omega^4 + a_1 \omega^3 + a_2 \omega^2 + (a_3 + i b_3) \omega + a_4 + i b_4 = 0 ; \tag{25}$$

where

$$\begin{aligned} a_1 &= 2(! + ! ) ; \\ a_2 &= (! + ! )^2 + 2(!_A^2 + ! ! ) + \frac{k_z^2}{k^2} \omega^2 + 4 \frac{k_z^2}{k^2} !_A^2 ; \\ a_3 &= 2(! + ! )(!_A^2 + ! ! ) + 2 \frac{k_z^2}{k^2} \omega^2 + \\ &\quad + 4 \frac{k_z^2}{k^2} (! + ! ) !_A^2 ; \\ a_4 &= (!_A^2 + ! ! )^2 - 4 \frac{k_z^2}{k^2} !_A^2 \omega^2 + \frac{k_z^2}{k^2} \omega^2 (!_A^2 + !^2) + \\ &\quad + 4 \frac{k_z^2}{k^2} ! ! !_A^2 ; \\ b_3 &= 8 \frac{k_z^2}{k^2} !_A !_A ; \\ b_4 &= 4 \frac{k_z^2}{k^2} !_A !_A (! + ! ) - 2 \frac{k_z^2}{k^2} !_A !_A (! ! ) ; \end{aligned} \tag{26}$$

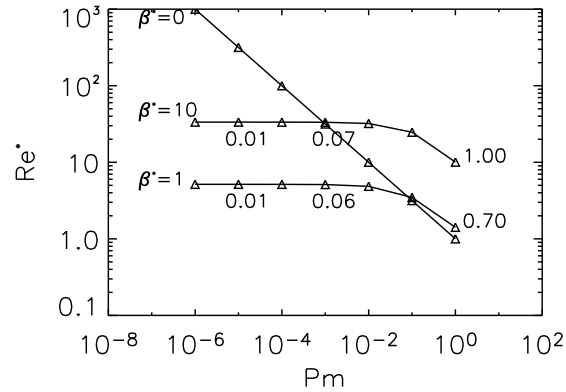


**Fig. 1** Rayleigh limit: Critical Reynolds number vs. magnetic Prandtl number for axial fields ( $\beta = 0$ ) and for helical fields ( $\beta > 0$ ). The curves are marked with the oscillation frequencies  $\omega$  which obviously do not depend on the  $\beta$ -values.

The dispersion relation (25) is now solved numerically for  $\omega = 0$ . To this end the (complex) frequency is again normalized with  $\frac{P}{P \frac{!}{!}}$ . Then from (26)

$$\begin{aligned} a_1 &= 2 \frac{P}{Pm} + \frac{1}{P \frac{!}{!}} ; \\ a_2 &= \frac{P}{Pm} + \frac{1}{P \frac{!}{!}} \omega^2 + 2 \omega (1 + Ha^2) + 4 \omega^2 Ha^2 ; \\ a_3 &= 2 \omega (1 + Ha^2) \frac{P}{Pm} + \frac{1}{P \frac{!}{!}} \omega + \\ &\quad + 4 \omega^2 Ha^2 \frac{P}{Pm} + \frac{1}{P \frac{!}{!}} \omega ; \\ a_4 &= (1 + Ha^2 \omega^2 - 4 Ha^2 Re^2 Pm + 4 \omega^2 Ha^2) ; \\ b_3 &= 8 \omega Ha^2 Re \frac{P}{Pm} ; \\ b_4 &= 4 \omega Ha^2 Re (1 + Pm) ; \end{aligned} \tag{27}$$

For given Pm,  $\omega$  and Ha the dispersion relation can be solved in the following way. For too small Re all the solutions of (25) will have negative  $\Re(\omega)$  so that the perturbations decay. For a certain Re, however, the first real part of one of the roots becomes positive so that the disturbance grows and the flow becomes unstable. Then this minimum Re is searched which provides the lowest Re. This minimum Re is shown in Fig. 1 for various  $\omega$  in its dependence on the magnetic Prandtl number. Also the resulting normalized frequencies  $\omega$  are given which indeed do not depend on  $\beta$ . Note the basic difference of the solution for  $\beta = 0$  and  $\beta > 0$ . Clearly for  $Pm \ll 0$  the solution with  $\omega = 0$  scales with  $Rm = Pm Re$  while the solutions with  $\omega > 0$  scale with Re. For  $Pm = 1$  no basic difference exists between the solutions as there is no difference between Re and Rm. The consequence of the different scalings for small magnetic Prandtl number is a rather small critical Re for  $\beta > 0$ .

One can also take from Fig. 1 that for  $\beta = 0$   $Re / Pm = 1$ . We know this relation as a particularity of the

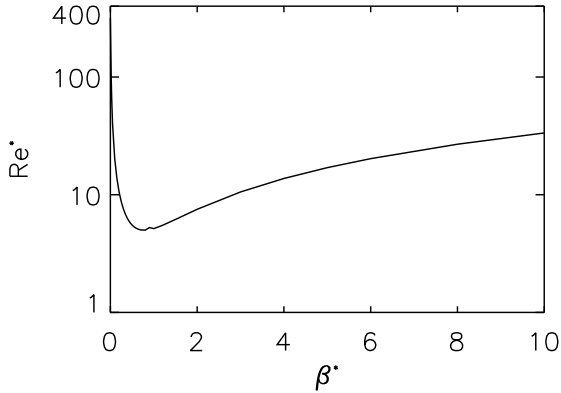


**Fig. 2** Rayleigh limit: Critical Reynolds numbers vs. toroidal field component  $\beta^*$  for fixed magnetic Prandtl number ( $P_m = 10^{-5}$ ). On the vertical axis:  $Re = 317$ ;  $Ha = 1$ .

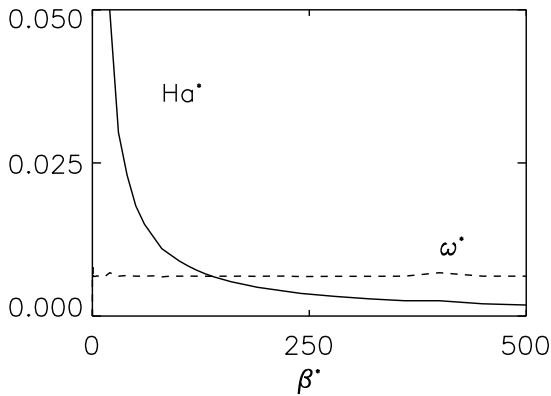


**Fig. 3** Rayleigh limit: Hartmann number and oscillation frequency for fixed magnetic Prandtl number ( $P_m = 10^{-5}$ ) for very strong toroidal field components. Note the constancy of  $\omega^*$  over the whole range of Reynolds numbers and pitch angles  $\beta^* > 0$ .

Rayleigh limit<sup>1</sup> which changes to  $Re_c = 1/P_m$  (i.e.  $R_m = \text{const}$ ) beyond the Rayleigh limit (see Rüdiger & Hollerbach 2004).

We now ask for the function  $Re = Re(\beta^*)$  for fixed and small  $P_m$ . Figure 2 shows the characteristic profile for  $P_m = 10^{-5}$ . A minimum Reynolds number exists for  $\beta^* \approx 0.5$  which is smaller by two orders of magnitude than  $Re_c$  for  $\beta^* = 0$ .

When the Reynolds number decreases for growing  $\beta^*$  the frequency  $\omega^*$  increases to the value  $\omega^* = P_m$  and remains then constant (see Eq. 24). For small  $P_m$  it does not depend on and/or  $Re$ . The amplitude confirms the basic result (22).

Beyond the minimum  $Ha = 1/P_m$  and  $Re = 1/P_m$  which can be observed in Fig. 2.

In summary, the MRI for the Rayleigh limit  $\beta^* < R^2$  exists for not too high ratios of azimuthal and axial magnetic field components. It is basically oscillating but not for

<sup>1</sup> It follows directly from the relation  $a_4 = 0$  for  $\beta^* = 0$ .

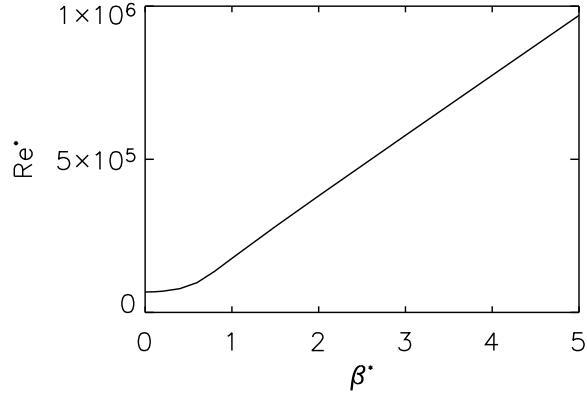


**Fig. 4** Kepler flow: The characteristic minimum in the Reynolds number profile disappears. The toroidal field component stabilizes the MRI. On the vertical axis:  $Re = 66670$ ;  $Ha = 259$ ,  $P_m = 10^{-5}$ .

the exceptional case of  $B = 0$ . The oscillation frequency approaches the viscous frequency  $\omega^* = P_m$ . Pitch angles of order ten strongly destabilize the MRI, there is a deep and wide trough in the profile  $Re = Re(\beta^*)$  as shown in Fig. 2. Note that for  $\beta^*$  of order ten the scaling with  $Re$  for  $P_m \neq 0$  still exists which is characteristic for HMRI.

### 5 Kepler flow: local solutions

In order to model the flat rotation law of a Kepler flow we have to work with (26) and  $\beta^* = \beta$ . The numerical results are shown in Fig. 4. They strongly differ from the results for the Rayleigh limit. The characteristic trough in the Reynolds number profile in Fig. 2 disappears. The toroidal field always stabilizes the MRI. After Fig. 4 the Reynolds number grows with  $\beta^*$ , i.e.

$$Re \propto \beta^{1/2} \quad (28)$$

There is no instability anymore with very small magnetic Reynolds number or small Lundquist number. Obviously, in the local approximation the solution in Fig. 1 which scales for  $P_m \neq 0$  with  $Re$  instead of  $R_m$  disappears for too flat rotation profiles.

For the resulting frequency  $\omega^*$  Fig. 5 provides  $\omega^* \approx 0.8 \omega_A$  independent of the pitch angle  $\beta^*$ . In units of the rotation frequency, however,

$$\omega^* / \Omega = 1 \quad (29)$$

This result depends on the pitch angle of the magnetic field but does not depend on the magnetic Prandtl number.

### 6 Global TC containers

With a local approximation we have considered the instability of differential rotation under the presence of a current-free magnetic field with helical geometry, i.e.  $B_z B_\theta \neq 0$ .

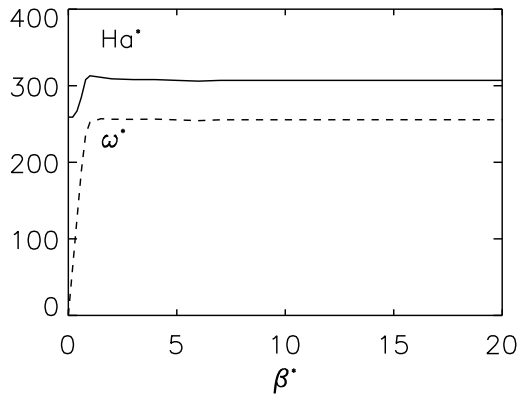


**Fig. 5** Kepler flow: The Hartmann number  $Ha^*$  and the oscillation frequency  $\omega^*$  are almost constant for  $\beta^* > 1$  and they are almost equal so that again  $\omega^* \approx 0.81 \cdot Pm = 10^5$ .

The local approximation only describes flows with an extremely small radial extension. The instability for such field geometries forms an overstable pattern of axisymmetric perturbations of flow and field. The corresponding eigenoscillation only vanishes for  $B = 0$ . Beyond the Rayleigh limit Lakhin & Velikhov (2007) find in the short-wave approximation that the eigenfrequency fulfills  $\omega^* \approx 0.81$  without any relation to the magnetic field.

The basically unknown quantity in local approximations is the resulting wave number  $k$ . We shall switch, therefore, to the consideration of global models where the wave number no longer is an unknown quantity. We shall find that the eigenoscillation  $\omega$  of HMRI equals the viscosity frequency also for global solutions for all pitch angles  $\beta$  but only at the Rayleigh line. For more flat rotation laws the resulting eigenfrequency of the HMRI modes proves to be fixed by the Alfvén frequency of the vertical field.

For comparison with the results of the local approximation we first consider a container with a small gap between the cylinders ( $R_{in} = R_{out} = 0.67$ ) which are assumed as *perfect conductors*. The rotation law between the cylinders is

$$\omega = a + \frac{b}{R^2}; \tag{30}$$

with

$$a = \frac{\omega_{in}}{1 - \beta^2}; \quad b = \frac{1}{1 - \beta^2} R_{in}^2 \omega_{in}; \tag{31}$$

where

$$\beta = \frac{R_{in}}{R_{out}}; \quad \omega_{in} = \frac{\omega_{out}}{\beta}; \tag{32}$$

$\omega_{in}$  and  $\omega_{out}$  are the imposed rotation rates of the inner and outer cylinders with their radii  $R_{in}$  and  $R_{out}$ . The Rayleigh limit is reached if  $\beta = \sqrt{2}$ , i.e.  $\beta = 0.44$  for the considered small-gap container. The axial field  $B_z$  is uniform while the toroidal field is current-free in the gap, i.e.  $B = B_z = R_{in} = R_{out}$ . The Hartmann number and

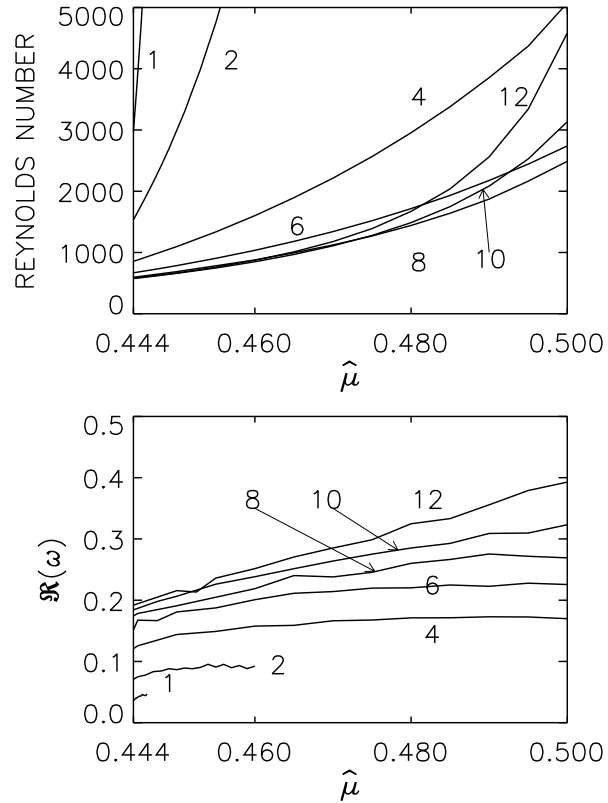


**Fig. 6** Reynolds number (*top*) and eigenfrequency (normalized with  $\omega_{in}$ , *bottom*) for a small-gap container ( $\beta = 0.67$ ) filled with gallium ( $Pm = 10^6$ ) vs. the rotation rate ratio  $\hat{\beta}$ . The vertical axis at the left represents the Rayleigh limit. The curves are marked with their  $Pm$ -values. Note the clear dependence of  $\omega = \omega_{in}$  on the pitch angle  $\hat{\beta}$ .

the Reynolds number are the dimensionless numbers of the problem,

$$Ha = \frac{B_z R_0}{\rho}; \quad Re = \frac{\omega_{in} R_0^2}{\nu}; \tag{33}$$

where  $R_0 = (R_{in} (R_{out} - R_{in}))^{1/2}$  is taken as the unit of length. We have used  $R_0^{-1}$  as the unit of the wave number and  $\omega_{in}$  as the unit of frequencies. We shall also use the magnetic Reynolds number  $Rm = Pm Re$ . Details of the numerics can be found in Rüdiger et al. (2007a,b) and references therein.

In Fig. 6 the Reynolds number (*top*) and the normalized oscillation frequency  $\omega = \omega_{in}$  (*bottom*) are given for very small magnetic Prandtl number ( $Pm = 10^6$ ) and for various values of  $\beta$ . The main result is that for larger  $\beta$  the critical Reynolds decreases and the normalized (!) oscillation frequency grows. In consequence, the product of Reynolds number and oscillation frequency  $\omega = \omega_{in}$  should not vary too much with the  $\beta$ -values (see Fig. 7, *top*). At the Rayleigh limit we indeed find one and the same value for the considered product independent of  $\beta$  leading back to (21) yielding the basic relation (22). At the Rayleigh line the oscillation frequency is thus exactly given by the viscosity frequency. This is not true, however, beyond the Rayleigh line. There

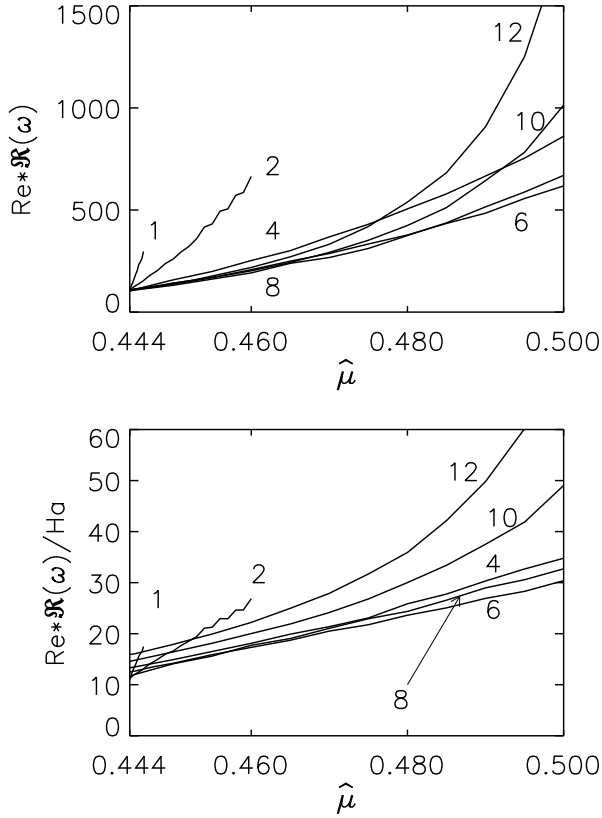


**Fig. 7** The same as in Fig. 6 but for the product of Reynolds number and eigenfrequency (*top*) and this product divided by Ha (*bottom*). Note that at the Rayleigh line the product of Reynolds number and eigenfrequency does not depend on  $\hat{\mu}$  and note that outside the Rayleigh line for medium  $\hat{\mu}$  the use of the magnetic normalization is successful.

we have the phenomenon that the oscillation frequency normalized with the viscosity frequency strongly depends on the  $\hat{\mu}$ -value (Fig. 7, top). However, the  $\hat{\mu}$ -dependence beyond the Rayleigh line is reduced if the Hartmann number of the axial field is used (Fig. 7, bottom). For (medium)  $\hat{\mu} \approx 4$ –8 the curves show  $Re \cdot \omega(\hat{\mu}) / Ha$  independent of  $\hat{\mu}$ . This means

$$\omega \approx \omega_A; \quad (34)$$

almost independent of  $\hat{\mu}$  for medium values of  $\hat{\mu}$ . A weak dependence on  $\hat{\mu}$  remains. Equation (34) means that for given magnetic Prandtl number the amplitude of the vertical field determines the oscillation frequency. This relation is not valid for too small nor too large values of  $\hat{\mu}$ . For too small  $\hat{\mu}$  the influence of the toroidal field is too weak and for too large  $\hat{\mu}$  the influence of the axial field is too weak.

## 7 Kepler flow: global solutions

In contrast to the previous results we have demonstrated with nonlocal calculations that even for Kepler rotation

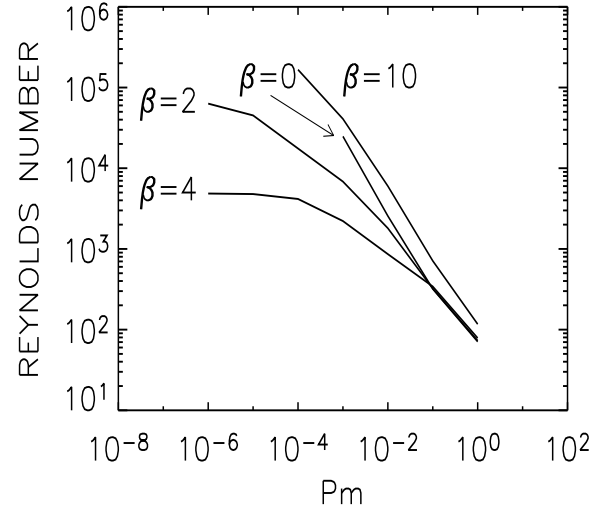


**Fig. 8** The critical Reynolds numbers for quasi-Kepler rotation. Note that the fields with  $\hat{\mu} = 0$  and  $\hat{\mu} = 10$  for  $Pm \neq 0$  scale with  $Rm$  and the fields with  $\hat{\mu} = 2$  and  $\hat{\mu} = 4$  scale with  $Re$ . Perfect conducting cylinders,  $m = 0$ ,  $\hat{\mu} = 0.5$ .

HMRI occurs if at least one of the boundaries is sufficiently conducting (Rüdiger & Hollerbach 2007). The short-wave method used in the foregoing sections does not reflect these results. In the following the Taylor-Couette calculations for flat rotation laws have been repeated i) to probe the basic results with another code and ii) to find more details about the dependence of this effect on the magnetic Prandtl number and about the eigenfrequencies and iii) to include nonaxisymmetric modes into the considerations. In order to obtain exact solutions we remain in the frame of the Taylor-Couette flows so that only quasi-Kepler rotation laws can be considered. A quasi-Kepler rotation law fulfills at both cylinders the Kepler law  $\omega / R^{1.5}$  so that the condition  $\omega = \hat{\mu}^{1.5}$  results. Here (as also in Rüdiger & Hollerbach 2007) with the standard gap of  $\hat{\mu} = 0.5$  is worked so that  $\omega = 0.35$  holds for the quasi-Kepler approximation.

The experiment PROMISE works with a rotation law with  $\omega = 0.27$ . The experimental setup utilizes the existence of the trough in the relation of  $Re$  and  $\hat{\mu}$  where the critical Reynolds number of the instability becomes very low. For more flat rotation laws one expects an increase of the critical Reynolds number. Lakhin & Velikhov (2007) have shown that for  $\hat{\mu} = 10$  an instability exists, with frequencies about one order of magnitude smaller than the basic rotation, but the trough for medium  $\hat{\mu}$ -values disappears. All the solutions are now scaling with  $Rm$  rather than with  $Re$ . We shall show, however, that this result does *not* reflect the situation in Kepler disks which obviously cannot be described in a local approximation.

Figure 8 gives the critical Reynolds numbers as a function of  $\hat{\mu}$  and  $Pm$ . It is clearly shown that for small  $\hat{\mu}$  ( $\hat{\mu} = 0$ ) and large  $\hat{\mu}$  ( $\hat{\mu} = 10$ ) the instability scales with  $Rm$  while for  $Pm \neq 0$  the instability for  $\hat{\mu} = 2$  and  $\hat{\mu} = 4$  scales with

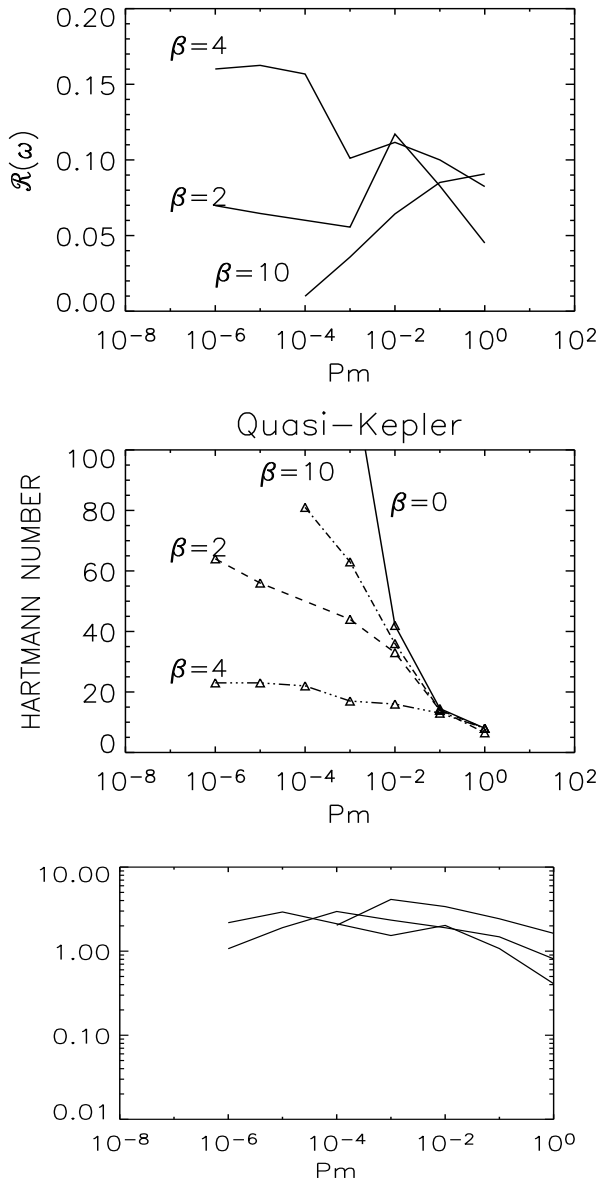


**Fig. 9** The normalized eigenfrequency ( $\omega = \omega_{in}$ , top), the critical Hartmann numbers (middle) and the numerical basis of Eq. (35) for quasi-Kepler rotation (bottom). In the bottom plot the curves are for  $\beta = 2; 4; 6$ . Parameters as in Fig. 8.

Re. This is the usual constellation for HMRI. For Kepler rotation there is no basic difference close to the Rayleigh line. For  $P_m = 1$  no distinction exists between Re and Rm so that all differences disappear between the solutions for different  $\beta$ . The oscillation frequencies  $\omega = \omega_{in}$  are of order 0.1 (with a weak  $\beta$ -dependence for small  $P_m$ ) and they only slightly depend on the magnetic Prandtl number (see Fig. 9, top). One finds

$$\frac{\omega}{\text{Re}} \frac{\text{Re}}{\text{Ha}} P_m^{1=4} \approx 1 \tag{35}$$

for  $P_m$  between  $10^{-6}$  and 1 (Fig. 9, bottom). Hence

$$\omega = \omega_A P_m^{1=4}; \tag{36}$$

independent of  $\beta$ . Only the amplitude of the axial field fixes the eigenfrequency. The influence of the magnetic Prandtl number is small. This is a numerical result for not too small  $P_m$ , the physical meaning of the  $P_m$ -factor is not yet completely clear. The result (36) for  $P_m = 10^{-5}$  is smaller by one order of magnitude than the result derived from the dispersion relation.

### 7.1 Nonaxisymmetric modes

Also nonaxisymmetric solutions with  $\exp(im\theta)$  have been computed with this model which represent solutions drifting along the azimuth. Rüdiger et al. (2005) find the solution of this problem for  $m = 1$  for various  $\beta$  but only for a fixed magnetic Prandtl number. Always the mode with  $m = 1$  needs a higher Reynolds number to be excited than the mode with  $m = 0$ . At the Rayleigh limit and for  $P_m = 10^{-5}$  the critical Reynolds number proves to be  $3 \cdot 10^4$

#### 7.1.1 Standard MRI

For standard MRI (i.e.  $\beta = 0$ , see Rüdiger & Zhang 2001; Ji, Goodman & Kageyama 2001) the calculations have been repeated for various magnetic Prandtl numbers and for  $m = 0; 1; 10$  (Fig. 10). For all nonvanishing  $m$  the critical Reynolds numbers lie above the curve for  $m = 0$ . It is also understandable that this effect grows for smaller Prandtl numbers. The differential rotation increases the magnetic dissipation of nonaxisymmetric patterns growing with  $m^2$  and runs with  $1=P_m$ . This situation exists for both steep rotation law (top) and also for flat rotation laws such as the Keplerian one (bottom). In general, the nonaxisymmetric modes are strongly stabilized, by the smoothing action of differential rotation but also by the appearance of the azimuthal drift as argued by Mikhailowskii et al. (2008). Standard MRI is obviously a basically axisymmetric phenomenon.

#### 7.1.2 HMRI

The motivation for the inclusion of nonaxisymmetric modes for helical magnetic geometry is that for large  $\beta$  the toroidal field dominates the axial field so that previous computations concerning the  $m = 1$  instability for azimuthal (current-free) magnetic fields with  $B_{\theta} / B_{\parallel} = R$  (AMRI) should be concerned. In Fig. 11 the dashed line gives the instability limit for  $\beta = 10$ . One finds that it scales with Rm for  $P_m \neq 0$  also known for AMRI (see Rüdiger et al. 2007b).

For the mode with  $m = 1$  the critical Reynolds number for small  $P_m$  exceeds the critical Reynolds number for  $m = 0$  so that the axisymmetric traveling-mode is *much easier* to excite than the nonaxisymmetric solution. The opposite is true for  $P_m > 10^3$ . In this case, for  $\beta = 10$ , the nonaxisymmetric modes are more easy to excite.

We also computed the nonaxisymmetric solutions for  $\beta = 2$  and  $\beta = 4$ . We find that their instability limits can not be distinguished from that for  $\beta = 10$ . It is clear that

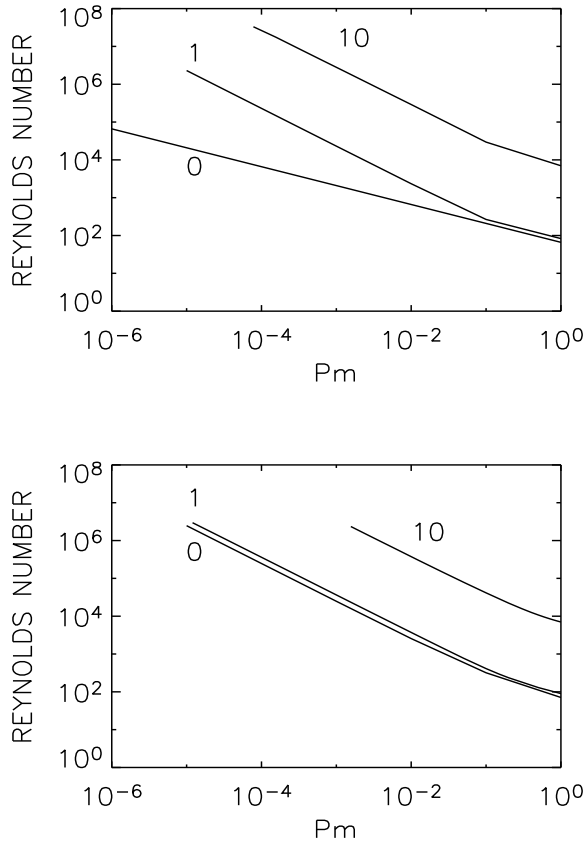


**Fig. 10** The critical Reynolds numbers for standard MRI (i.e.  $\beta = 0$ ) vs. magnetic Prandtl number at the Rayleigh limit (*top*) and for quasi-Kepler rotation (*bottom*). The curves are marked with their mode number  $m$ . In both cases for small  $Pm$  the differences are huge.

also the solutions with  $\beta > 10$  comply with the curve for  $\beta = 10$ . The Hartmann number, however, becomes smaller and smaller for growing  $\beta$  which, however, is not a surprise as for azimuthal MRI (also for the Tayler instability) the toroidal field strength is important, i.e. the product  $\beta H a$ .

Note that for small  $Pm$  the Hartmann numbers for  $m = 1$  are *much* higher than for  $m = 0$  (Fig. 12). This may be a simple consequence of the fact that AMRI scales with the Lundquist number  $S = \frac{\beta}{Pm} H a$ .

## 7.2 Results

The basic results from our calculations for quasi-Keplerian rotation laws are:

1. For  $0 < \beta < 4$  and  $Pm < 1$  the axisymmetric HMRI has always the lowest Reynolds number. The traveling-wave solution with  $m = 0$  which is observed in the PROMISE experiment forms the instability which is most easiest to excite also for Kepler rotation. Opposite statements (Liu et al. 2006) cannot be confirmed.
2. The oscillation frequency for  $\beta > 0$  equals the viscosity frequency but only at the Rayleigh line. For quasi-

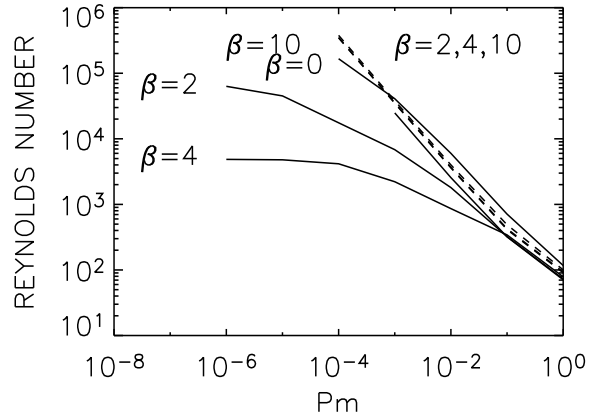


**Fig. 11** The same as in Fig. 8 but with the nonaxisymmetric mode  $m = 1$  included. The solid lines give the axisymmetric modes ( $m = 0$ ) for various  $\beta$  while the dashed line belongs to the nonaxisymmetric ( $m = 1$ ) modes for all  $\beta$ .

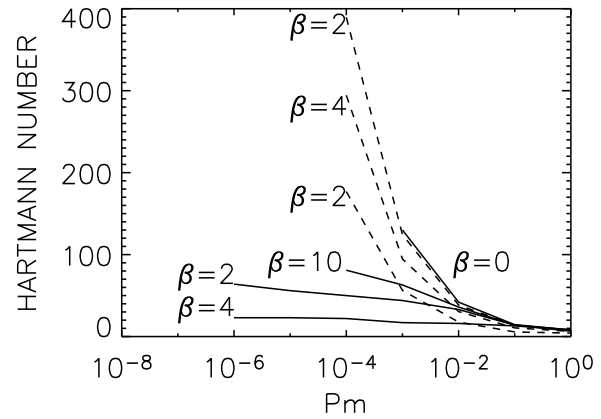


**Fig. 12** The same as in Fig. 11 but for the Hartmann number.

Kepler rotation it proves to be the Alfvén frequency of the vertical magnetic field.

3. For larger  $\beta$  ( $\beta > 10$ ) and  $Pm < 10^{-3}$  the lowest Reynolds numbers belong to the axisymmetric HMRI while for  $Pm > 10^{-3}$  they always belong to the nonaxisymmetric AMRI.
4. The neutral instability line for  $m = 1$  does not depend on  $\beta$ , i.e. the AMRI is not concerned by the existence of axial fields.

The calculations demonstrate the strong influence of the magnetic Prandtl number for the MHD instability theory. The formula SMRI (axisymmetric, stationary, scaling with  $Rm$ ) + AMRI (nonaxisymmetric, drifting, scaling with  $Rm$ ) = HMRI (axisymmetric, oscillating, scaling with  $Re$ ) exists only for small  $Pm$ .

## References

- Blokland, J.W.S., van der Swaluw, E., Keppens, R., Goedbloed, J.P.: 2005, *A&A* 444, 337  
 Elstner, D., Rüdiger, G., Tschäpe, R.: 1989, *GAJFD* 48, 235  
 Hollerbach, R., Rüdiger, G.: 2005, *Phys Rev Lett* 95, 124501



- Ji, H., Goodman, J., Kageyama, A.: 2001, MNRAS 325, L1  
Knobloch, E.: 1996, PhFl 8, 1446  
Lakhin, V.P.: 2007, private communication  
Lakhin, V.P., Velikhov, E.P.: 2007, PhLA 369, 98  
Liu, W., Goodman, J., Herron, I., Ji, H.: 2006, Phys Rev E 74, 6302  
Mikhailovskii, A.B., Lominadze, J.G., Churikov, A.P., et al.: 2008, PPCF 50, 085012  
Rüdiger, G., Hollerbach, R.: 2004, *The Magnetic Universe*, Wiley-VCH, Weinheim  
Rüdiger, G., Hollerbach, R.: 2007, Phys Rev E 76, 068301  
Rüdiger, G., Zhang, Y.: 2001, A&A 378, 302  
Rüdiger, G., Hollerbach, R., Schultz, M., Shalybkov, D.A.: 2005, AN 326, 409  
Rüdiger, G., Hollerbach, R., Gellert, M., Schultz, M.: 2007a, AN 328, 1158  
Rüdiger, G., Hollerbach, R., Schultz, M., Elstner, D.: 2007b, MNRAS 377, 1481  
Velikhov, E.P., Ivanov, A.A., Lakhin, V.P., Serebrennikov, K.S.: 2006, PhLA 356, 357